www.elsevier.com/locate/jssc

Magnetic order and crystal structure study of YNi_4Si-type $NdNi_4Si$

Jinlei Yao, O. Isnard, A.V. Morozkin, T.I. Ivanova, Yu. S. Koshkid'ko, A.E. Bogdanov, S.A. Nikitin, W. Suski

PII: S0022-4596(14)00495-2
DOI: http://dx.doi.org/10.1016/j.jssc.2014.11.016
Reference: YJSSC18708

To appear in: *Journal of Solid State Chemistry*

Received date: 3 October 2014
Revised date: 11 November 2014
Accepted date: 16 November 2014

Cite this article as: Jinlei Yao, O. Isnard, A.V. Morozkin, T.I. Ivanova, Yu. S. Koshkid'ko, A.E. Bogdanov, S.A. Nikitin, W. Suski, Magnetic order and crystal structure study of YNi_4Si-type $NdNi_4Si$, *Journal of Solid State Chemistry*, http://dx.doi.org/10.1016/j.jssc.2014.11.016

Magnetic order and crystal structure study of YNi_4Si-type $NdNi_4Si$

Jinlei Yao [a], O. Isnard [b,c], A. V. Morozkin [d,*], T.I. Ivanova [e], Yu. S. Koshkid'ko [f,g], A. E. Bogdanov [e], S. A. Nikitin [e], W. Suski [f,h]

[a] *Research Center for Solid State Physics and Materials, School of Mathematics and Physics, Suzhou University of Science and Technology, Suzhou 215009, China*

[b] *Université Grenoble Alpes, Inst NEEL, BP166, Grenoble F-38042, France*

[c] *CNRS, Institut NEEL, 25 rue des martyrs, Grenoble F-38042, France*

[d] *Department of Chemistry, Moscow State University, Leninskie Gory, House 1, Building 3, Moscow, GSP-2, 119992, Russia*

[e] *Physics Department, Moscow State University, Moscow 119992, Russia*

[f] *International Laboratory of High Magnetic Fields and Low Temperatures, Wrocław, Poland*

[g] *VSB-Technical University of Ostrava, Ostrava-Poruba 70833, Czech Republic*

[h] *Polish Academy of Sciences, Trzebiatowski Institute of Low Temperatures and Structure Research, P.O. Box 1410, 50-950 Wrocław 2, Poland*

Abstract

Magnetic measurements and neutron powder diffraction investigation of the magnetic structure of the orthorhombic YNi_4Si-type (space group *Cmmm*) $NdNi_4Si$ compound are presented. The magnetocaloric effect of $NdNi_4Si$ is calculated in terms of the isothermal magnetic entropy change and it reaches the maximum value of –3.3 J/kg·K for a field change of 50 kOe near T_C = 12 K. Below ~12 K, $NdNi_4Si$ exhibits a commensurate *b*-axis collinear ferromagnetic ordering with the ***Cmm′m*** magnetic space group in a zero magnetic field. At 1.5 K, the neodymium atoms have the magnetic moment of 2.37(5) μ_B. The orthorhombic crystal structure and its thermal evolution are discussed in comparison with the $CaCu_5$-type compound.

Keywords: Rare-earth compounds; Magnetic properties; Magnetocaloric effect; Neutron diffraction; Magnetic structure

*Corresponding author. E-mail address: morozkin@tech.chem.msu.ru (A.V. Morozkin).

1. Introduction

Recently, the orthorhombic derivative of the $CaCu_5$-type, namely the YNi_4Si-type (space group *Cmmm*), RNi_4Si compounds (R = Y, La, Ce, Sm, Gd - Ho) were reported [1]. These compounds supplement the known series of the $CaCu_5$-type RNi_5 compounds and RNi_4Si solid solutions [2, 3]. The orthorhombic distortion of parent $CaCu_5$-type compounds may be considered a prospective route for optimizing their magnetic and hydrogen storage properties [4-6]. In order to test its feasibility, it requires a systematic investigation of the magnetic properties of YNi_4Si-type RNi_4Si, which can be in comparison with those of the well-known $CaCu_5$-type RNi_5 and RNi_4Si compounds.

The early reports of the magnetic properties and structures of $CaCu_5$-type RNi_5 and RNi_4Si [7-11] and YNi_4Si-type RNi_4Si [1, 12, 13] (R = Gd, Tb, Dy) permit us to draw the following preliminary conclusions. In the case of {Tb, Dy}Ni_4Si the ferromagnetic ordering temperature increases from the $CaCu_5$-type RNi_5 across $CaCu_5$-type RNi_4Si to YNi_4Si-type RNi_4Si, whereas the Curie point decreases from $GdNi_5$ to the $CaCu_5$-type $GdNi_4Si$ and the Curie temperatures of $CaCu_5$-type and YNi_4Si-type $GdNi_4Si$ are the same. We suggest that the transformation of their magnetic properties in the orthorhombic distortion of $CaCu_5$-type lattice results from the initial *ab*-plane ferromagnetic-like ordering of Tb and Dy sublattices and possible *c*-collinear ferromagnetic ordering of Gd sublattice. The Ni ions have little to no magnetic moments in these compounds.

The initial $CaCu_5$-type $NdNi_5$ shows ferromagnetic ordering below 7.2 K with isothermal magnetic entropy change of –8.45 J/kg•K for a field change of 0-50 kOe [14, 15]. The substitution of Si for Ni in the $NdNi_4Si$ solid solution leads to increasing of Curie point from 7.2 to 9.2 K and decreasing of isothermal magnetic entropy change from –8.45 J/kg•K to -7.3 J/kg•K for a field change of 0-50 kOe [16].

This work aims to understand the effects of orthorhombic distortion from the parent $CaCu_5$-type $NdNi_5$ to the YNi_4Si-type $NdNi_4Si$ compound through the magnetic measurements and neutron powder diffraction.

2. Material and methods

The $NdNi_4Si$ sample was prepared by arc melting of the stoichiometric amounts of Nd (99.9 wt. %), Ni (99.95 wt. %) and Si (99.99 wt. %). The sample was annealed at 1070 K for 200 h in an argon-filled and sealed quartz tube and subsequently quenched in ice-cold water. The structure, purity and composition of the polycrystalline sample were evaluated using powder X-ray diffraction (XRD) and electron microprobe analysis. The XRD data were obtained on a Rigaku D/MAX-2500 diffractometer ($CuK_{\alpha 1}$ radiation, 2θ = 10 - 80 deg, step 0.02 deg, 1 s/step). An INCA-Energy-350 X-ray EDS spectrometer (Oxford Instruments) on the Jeol JSM-6480LV scanning electron microscope (20 kV accelerating voltage, beam current 0.7 nA and beam diameter 50 micron) was employed to perform the microprobe analyses of the sample. Signals from three points were averaged and estimated standard deviations were 1 at. % for Nd (measured by L-series lines), 1 at. % for Ni and 1 at. % for Si (measured by K-series lines).

DC magnetization of the polycrystalline $NdNi_4Si$ sample was measured on a commercial Physical Property Measurement System (Quantum Design PPMS-DynaCool) in the temperatures range of 5 - 300 K with an applied magnetic field of 5 kOe in the zero-field-cooled (ZFC) and field-cooled (FC) modes. The isothermal saturation magnetization was measured for the magnetic field change from 0 to 50 kOe at various temperatures.

Neutron diffraction experiments were carried out at the high flux reactor of the Institut Laue Langevin (Grenoble, France). The data were collected in a zero magnetic field on the two-axis D1B powder diffractometer equipped with a 1300 cell curved detector spanning the 2θ range of 130 deg. [17]. The temperature ranges were 128 K – 30 K with a step of ~10 K and 25 K – 1.5 K with a step of ~

5 K. The neutron wavelength of 2.5238 Å was selected by the (002) reflection of a pyrolitic graphite monochromator and the 2θ step was 0.1 deg.

3. Theory/calculation

The unit cell data were derived from the powder XRD using the Rietan program [18, 19] in the isotropic approximation at room temperature. The paramagnetic susceptibility was fitted to the Curie-Weiss law to obtain the effective magnetic moment and paramagnetic Curie temperature [20]. Magnetocaloric effect (MCE) was calculated in terms of the isothermal magnetic entropy change, ΔS_m, using the magnetization vs. field data obtained near the magnetic transition and employing the thermodynamic Maxwell equations [21]. The neutron diffraction data were refined with the FULLPROF program [22]. The magnetic space groups [23, 24] were used for the analysis of neutron diffraction data.

4. Results

4.1. Crystal structure

Both the microprobe and X-ray powder analyses show that $NdNi_4Si$ is a single-phase sample. The microprobe analysis yielded the $Nd_{17(1)}Ni_{68(1)}Si_{15(1)}$ composition, and the X-ray powder analysis confirmed the YNi_4Si-type structure with the *Cmmm* space group. The lattice parameters were refined as a = 0.51354(2) nm, b = 0.83006(3) nm, c = 0.39707(2) nm, V = 0.16926(4) nm^3, $b/(3^{1/2}\cdot a)$ = 0.93320(3), and the atomic sites Nd (2*a*) [0, 0, 0], Ni1 (4*i*) [0, 0.3424(5), 0], Ni2 (4*f*) [1/4, 1/4, 1/2] and Si (2*c*) [0, 1/2, 1/2] (R_F = 4.5 %). The atomic positions for the Nd 2*a,* Ni1 4*i* and Ni2 4*f* sites in the *Cmmm* space group with the corresponding symmetry operators are given in **Table 1**.

4.2. Magnetic properties and magnetocaloric effect

The zero-field-cooled (ZFC) and field-cooled (FC) magnetization data recorded during heating in 5 kOe are shown in **Fig. 1a**. The FC data are indicative of a typical ferromagnet, while the ZFC data suggest presence of weak competing antiferromagnetic interactions, which can be easily overcome in

small magnetic fields. The paramagnetic susceptibility of $NdNi_4Si$ follows the Curie-Weiss law in the temperature range 90-300 K (inset in **Fig. 1a**). The fit to the Curie-Weiss law yielded a paramagnetic Weiss temperatures Θ_p = -21(5) K and the effective moment per formula unit M_{eff} = 3.8 μ_B/f.u. The negative Θ_p can be seen as the development of antiferromagnetic-type interactions, which is also observed in the ferromagnetic $SmNi_4Si$ compound [25]. The refined M_{eff} is close to the theoretical magnetic moment of Nd^{3+} (3.62 μ_B) [26], indicating Nd is trivalent in the compound. However the neutron diffraction studies do not confirm the presence of magnetic moments on Ni, and thus only Nd atoms are assumed to carry localized magnetic moments. In this case, the effective magnetic moment of the Nd atoms is 3.8 μ_B, and a slight increase of ~0.2 μ_B over the theoretical value can be attributed to the polarization of conduction electrons, predominantly the Nd 5*d* ones, through the 4*f*– 5*d* exchange interactions.

The magnetization *vs* magnetic field for $NdNi_4Si$ at 2 K is plotted in **Fig. 1b**. A rapid increase in the magnetization at low fields is typical for a ferromagnet and is attributed to the domain growth. However, a subsequent slow linear increase and non-saturating behavior is indicative of the competing antiferromagnetic interactions and/or strong anisotropy. A strong magnetic anisotropy is likely to be present in the $NdNi_4Si$ structure and does not allow the magnetic moments to be fully oriented in the magnetic field. The saturation magnetic moment reaches the value of 1.1 μ_B/Nd in 50 kOe, which is significantly smaller than the theoretical saturation moment 3.27 μ_B of Nd^{3+} [26]). $NdNi_4Si$ shows the hysteresis at 2 K with residual magnetisation M_{res} = 0.8 μ_B/fu and coercive field H_{coer} = 3.4 kOe (**Fig. 1b**). Existence of significant coercivity in the hysteresis cycle may be an indication of the presence of uniaxial magnetic anisotropy in the $NdNi_4Si$ compound, which is verified as a ferromagnetic ordering along the *b* axis through the neutron diffraction studies below.

The magnetocaloric effect of $NdNi_4Si$ in terms of the isothermal magnetic entropy change, ΔS_m, was calculated from the saturation magnetization data (**Fig. 2a**). A numerical integration is performed

using the following formula $\Delta S(T)_{mag} = \sum_i \frac{M_{i+1} - M_i}{T_{i+1} - T_i} \Delta H$, where ΔH is a magnetic field step and M_i and M_{i+1} are the values of magnetization at temperatures T_i and T_{i+1}, respectively [21]. The magnetic entropy change, ΔS_m, for ΔH = 0–50 kOe is plotted in **Fig. 2b**. As expected for a second order magnetic transition, ΔS_m peaks around the Curie temperature and has a maximum value of –3.3 J/kg·K.

4.3. Magnetic structure.

Above 10 K, the neutron diffraction patterns of $NdNi_4Si$ in a zero applied field correspond to the paramagnetic state, and at $T_C^{ND} \sim 10$ K a set of commensurate magnetic reflections with a $\mathbf{K}_0 = [0, 0, 0]$ wave vector indicates the magnetic ordering of $NdNi_4Si$ (**Fig. 3**). The ordering temperature found from the neutron diffraction study is in good agreement with the value deduced from the magnetisation measurements of $T_C \sim 12$ K (**Figs. 1a** and **4a**).

A commensurate *b*-axis collinear ferromagnetic model of $NdNi_4Si$ fits best with the NDP data (**Fig. 5**). Within this model, the calculated magnetic moments for the Ni1 and Ni2 sublattices are close to or within the error bar with $M_{Ni} \sim 0.13(15)$ μ_B, which means that the significance of such ordered magnetic moment on Ni can not be confirmed. The other tested commensurate variants yielded no magnetic ordering for the Ni sublattices either. The negligibile presence of the Ni magnetic moments in this compound results most probably from the Ni-3d band filling via electronic hybridization with the Nd and Ni neighbor states. The *b*-collinear magnetic ordering of the Nd sublattice corresponds to the ***Cmm′m*** magnetic space group as shown in **Table 1**. The neodymium magnetic moment reaches 2.37(5) μ_B at 1.5 K, a value less than the theoretical value of 3.27 μ_B expected for Nd magnetic moment [26] (**Fig. 4b** and **Table 2**), which is often obeserved in some rare-earth-based intermetallic compounds [27, 28].

The unit cell of $NdNi_4Si$ undergoes anisotropic distortion down to the ferromagnetic transition temperature: the cell parameters decrease with $a_T/a_{298} < b_T/b_{298K} < c_T/c_{298K}$, and below the ferromagnetic ordering the cell parameters remain almost constant (**Fig. 4c** and **Table 2**). As the

$NdNi_4Si$ structure is an orthorhombically distorted variant of the hexagonal $CaCu_5$ structure, the $b/3^{1/2}\cdot a$ ratio can be used to estimate the degree of the distortion and its progression with temperature. The $b/3^{1/2}\cdot a$ ratio stays almost constant from 298 K to 1.5 K and it is far from the unit value that corresponds to the transformation from the orthorhombic YNi_4Si-type lattice to the hexagonal $CaCu_5$-type lattice.

5. Discussion

The saturation magnetization at 2 K and in 50 kOe yielded a magnetic moment of 1.1 μ_B per neodymium atom (**Fig. 1b**), whereas neutron diffraction studies at 1.5 K and in a zero applied field indicated a complete ferromagnetic ordering of $NdNi_4Si$ with 2.37 μ_B/Nd (**Fig. 4b**). It can be understood that a large magnetic anisotropy prevents a parallel alignment of all the Nd moments in the polycrystalline sample with the magnetic field even at 50 kOe.

M. Falkowski et al. [16] reported the magnetic properties of $CaCu_5$-type $NdNi_4Si$ compound unfortunately without providing crystal data. Based on the aforementioned structural and magnetic data, we propose that transformation from the initial $CaCu_5$- to the YNi_4Si-type $NdNi_4Si$ unit cell (compression along the *b*-orthorhombic axis as in $TbNi_4Si$ [12]) leads to the modification in the Nd environment and thus the changes in their magnetic properties, such as, increasing of temperature of magnetic ordering from 9.2 K up to 12 K, reorientation the neodymium moments in the *ab*-plane normal to the compression of unit cell, decreasing of magnetocaloric effect from –7.3 J/kg·K of $CaCu_5$-type $NdNi_4Si$ down to –3.3 J/kg·K of YNi_4Si-type $NdNi_4Si$ in field of 0-50 kOe as in $TbNi_4Si$ [12]. Such a transformation leads to the appearance of distinct hysteresis loop at 2 K of the YNi_4Si-type $NdNi_4Si$ in contrast with the $CaCu_5$-type $NdNi_4Si$ (**Table 3**).

6. Conclusions

The new YNi_4Si-type $NdNi_4Si$ supplements the series of YNi_4Si-type RNi_4Si compounds with *R* = Y, La, Ce, Sm, Gd – Ho. Compared to the $CaCu_5$-type $NdNi_4Si$ compound, the YNi_4Si-type counterpart has the relatively high ferromagnetic ordering temperature (9.2 K vs. 12 K), the small magnetocaloric

effect (–7.3 J/kg·K vs. –3.3 J/kg·K for ΔH=50 kOe), and the large magnetic anisotropy at low temperatures. This work suggests that such an orthorhombic distortion from the initial $CaCu_5$-type unit cell can take place in the other YNi_4Si-type solid solutions, e.g., $PrNi_4Si$. The orthorhombic distortion may be used as a prospective route for optimisation of permanent magnetic properties in the family of $CaCu_5$-type rare earth materials.

Acknowledgements

This work was supported by the Russian Fund for Basic Research (Grant Nos. 12-03-00428-a and 13-02-00916), the National Natural Science Foundation of China (Grant No. 51301116), and the Natural Science Foundation of Jiangsu Province (Grant No. BK20130261). The Institute Laue Langevin (Grenoble, France) is warmly acknowledged for the use of the neutron diffraction beam. Y.S.K thank "Regional Materials Science and Technology Centre - Feasibility Program" of Czech Republic under Grant Nos. CZ.1.07/2.3.00/30.0016 and LO1203 for financial support.

.

References

[1] A.V. Morozkin, A.V. Knotko, V.O. Yapaskurt, Fang Yuan, Y. Mozharivskyj, R. Nirmala, J. Solid State Chem. 208 (2013) 9-13.

[2] P. Villars, L.D. Calvert, Pearson's Handbook of Crystallographic Data for Intermetallic Phases, ASM International, Materials Park, Ohio, 1985.

[3] SpringerMaterials The Landolt-Börnstein Database - Materials Science Data for 250000 Substances. http://www.springermaterials.com.

[4] K.J. Strnat, Ferromagnetic Materials, in: 131th ed., in: E.P. Wohlfarth, K.H.J. Buschow (Eds.), Elsevier Science, North-Holland, Amsterdam, 1988.

[5] E. Burzo, A. Chelkowski, H.R. Kirchmayr, Magnetic Properties of Metals, 248th ed., Springer-Verlag, Landolt-Вцrnstein, 1990.

[6] S.N. Klyamkin, V.N. Verbetsky, A.A. Karih, J. Alloys Compd. 231 (1995) 479-482.

[7] T. Tolinski, M. Falkowski, K. Synoradzki, A. Hoser, N. Stuber, J. Alloys Compd. 523 (2012) 43-48.

[8] N. Bucur, E. Burzo, R. Tetean, J. Optoelectron. Adv. Mater. 10 (2008) 801.

[9] M. Falkowski, B. Andrzejewski, A. Kowalczyk, J. Alloys Compd. 442 (2007) 155-157.

[10] L. Morellon, P.A. Algarabel, M.R. Ibarra, A.D. Moral, D. Gignoux, D. Schmitt, J. Magn. Magn. Mater. 153 (1996) 17.

[11] G. Aubert, D. Gignoux, B. Hennion, B. Michelutti, A.N, Saada, Solid State Commun. 37 (1981) 741-743.

[12] A.V. Morozkin, F. Yuan, Y. Mozharivskyj, O. Isnard, J. Magn. Magn. Mater. 368 (2014) 121-125.

[13] A.V. Morozkin, R. Nirmala, S.K. Malik, Magnetism and magnetocaloric effect in YNi_4Si-type RNi_4Si (R = Ce, Gd, Tb and Dy) compounds (submitted to J. Magn. Magn. Mater.)

[14] R.J. Radwanski, N.H.K. Ngan, J. Alloys Compd. 219 (1995) 260-263.

[15] P.J. von Ranke, M.A. Mota, D.F. Grangeia, A.M.G. Carvalho, F.C.G. Gandra, A.A. Coelho, A. Caldas, N.A. de Oliveira, S. Gama, Phys. Rev. B 70 (2004) 134428.

[16] M. Falkowski, T. Tolinski, A. Kowalczyk, Acta Phys. Pol. A 121 (2012) 1290-1292.

[17] www.ill.eu, Yellow Book.

[18] F. Izumi, in: R.A. Young (Ed.), The Rietveld Method, Oxford University Press, Oxford, 1993, p. 13.

[19] F. Izumi, Rigaku J. 6 (1989) 10.

[20] R.A. Levy, Principles of Solid State Physics, Academic Press, New York, 1968.

[21] A.M. Tishin, Y.L. Spichkin, The Magnetocaloric Effect and Its Applications, Institute of Physics Publishing, Bristol, Philadelphia, 2003, p. 480.

[22] J. Rodriguez-Carvajal, Physica B 192 (1993) 55-69.

[23] C.J. Bradley, A.P. Cracknell, The Mathematical Theory of Symmetry in Solids, Clarendon, Oxford 1972.

[24] D.B. Litvin, Magnetic Group Tables, 1-, 2- and 3-Dimensional Magnetic Subperiodic Groups and Magnetic Space Groups, International Union of Crystallography, 2013.

[25] M. Falkowski, M. Pugaczowa-Michalska, A. Kowalczyk, J. Alloys Compd. 577 (2013) 19-24.

[26] S. Legvold, Rare Earth Metals and Alloys, in: E.P. Wohlfarth (Ed.), Ferromagnetic Materials (North-Holland Publishing Company, Amsterdam, 1980, pp. 183-295.

[27] C. Chacon, O. Isnard, S. Miraglia, J. Alloys Compd. 283 (1999) 320-326.

[28] C. Zlotea, C. Chacon, O. Isnard, J. Appl. Phys. 92 (2002) 7382.

Figure Captions

Fig. 1. (a) Magnetization and inverse magnetic susceptibility of $NdNi_4Si$ as a function of temperature in 5 kOe and (b) magnetization vs. magnetic field of $NdNi_4Si$ at 2 K.

Fig. 2. (a) Magnetization vs. magnetic field and (b) the isothermal entropy change, $-\Delta S_m$, of $NdNi_4Si$ around the magnetic transition.

Fig. 3. Neutron diffraction patterns of $NdNi_4Si$ (a) at 25 K (paramagnetic state) and (b) at 1.5 K (*b*-axis ferromagnet with $\mathbf{K}_0$ = [0, 0, 0] wave vector. The first row of ticks refers to the nuclear Bragg peaks whereas the second row of lines refers to the magnetic reflections. The (hkl) of strongest magnetic reflections are indicated in **Figure 3b**.

Fig. 4. Thermal evolution of (a) strongest magnetic reflections $I_{(HKL)}$ in the neutron diffraction patterns of $NdNi_4Si$, (b) the magnetic moments of Nd atom (along *b* axis) and (c) of relative cell parameters

a_T/a_{298K}, b_T/b_{298K} and c_T/c_{298K}. Here a_T, b_T, c_T, a_{298K}, b_{298K} and c_{298K} are cell parameters of $NdNi_4Si$ at a given temperature T and 298 K, respectively.

.

Fig. 5. The magnetic structure of YNi_4Si-type $NdNi_4Si$ with *b*-axis collinear ferromagnetic ordering of Nd sublattice below ~12 K of ***Cmm′m*** magnetic space group ($\mathbf{K}_0$ = [0, 0, 0] wave vector).

Table 1.

Atomic positions for the 2*a*, 4*i* and 4*f* sites of the *Cmmm* [a-] space group (retained by $NdNi_4Si$) with the corresponding symmetry operators and magnetic space group ***Cmm′m*** [b-] (retained by *b*-axis collinear ferromagnetic ordering of $NdNi_4Si$) with corresponding magnetic symmetry operators.

Site	Atom	x/*a*	y/*b*	z/*c*	Symmetry operator	Magnetic symmetry operator
2*a*	Tb^1	0	0	0	*Pmmm* [c-]	***Pmm′m*** [f-]
	Tb^2	1/2	1/2	1/2	*Pmmm*/[1/2 0 1/2]	***Pmm′m*** × **1**/[1/2 0 1/2]
4*i*	$Ni1^1$	0	y	0	*Pm2m* [d-]	***Pm2m*** [–g]
	$Ni1^2$	0	-y	0	$\{\mathbf{2}_x, \mathbf{m}_y, \mathbf{2}_z, \bar{\mathbf{1}}\}$	$1' \times \{\mathbf{2}_x, \mathbf{m}_y, \mathbf{2}_z, \bar{\mathbf{1}}\}$
	$Ni1^3$	1/2	1/2+y	0	*Pm2m*/[1/2 1/2 0]	***Pm2m*** × **1**/[1/2 1/2 0]
	$Ni1^4$	1/2	1/2-y	0	$\{\mathbf{2}_x, \mathbf{m}_y, \mathbf{2}_z, \bar{\mathbf{1}}\}$/[1/2 1/2 0]	$1' \times \{\mathbf{2}_x, \mathbf{m}_y, \mathbf{2}_z, \bar{\mathbf{1}}\}$/[1/2 1/2 0]
4*f*	$Ni2^1$	1/4	1/4	1/2	$P2_1/n$ [e-]	$\boldsymbol{P2_1'/n}$ [h-]
	$Ni2^2$	-1/4	1/4	1/2	$\{\mathbf{m}_x, \mathbf{2}_x/[1/2\ 1/2\ 0], \mathbf{2}_y, \mathbf{m}_y/[1/2\ 1/2\ 0]\}$	$\{\mathbf{m}_x, 1' \times \mathbf{2}_x/[1/2\ 1/2\ 0], \mathbf{2}_y, 1' \times \mathbf{m}_y/[1/2\ 1/2\ 0]\}$
	$Ni2^3$	1/4	-1/4	1/2	$\{\mathbf{m}_x/[1/2\ 1/2\ 0], \mathbf{2}_x, \mathbf{2}_y/[1/2\ 1/2\ 0], \mathbf{m}_y\}$	$\{\mathbf{m}_x/[1/2\ 1/2\ 0], 1' \times \mathbf{2}_x, \mathbf{2}_y/[1/2\ 1/2\ 0], 1' \times \mathbf{m}_y\}$
	$Ni2^4$	-1/4	-1/4	1/2	$P2_1/n$/[1/2 1/2 0]	$\boldsymbol{P2_1'/n}$/[1/2 1/2 0]

[a-] $Cmmm = \{\mathbf{1}, \mathbf{m}_x, \mathbf{m}_y, \mathbf{m}_z, \bar{\mathbf{1}}, \mathbf{2}_x, \mathbf{2}_y, \mathbf{2}_z\} \times \{\mathbf{1}, \mathbf{1}/[1/2, 1/2, 0]\} = Pmmm \times \{1, 1/[1/2, 1/2, 0]\}$;

[b-] $\boldsymbol{Cmm'm} = \{\mathbf{1}, \mathbf{m}_x, 1' \times \mathbf{m}_y, \mathbf{m}_z, 1' \times \bar{\mathbf{1}}, 1' \times \mathbf{2}_x, \mathbf{2}_y, 1' \times \mathbf{2}_z\} \times \{\mathbf{1}, \mathbf{1}/[1/2, 1/2, 0]\} = \{\mathbf{1}, \mathbf{m}_x, \mathbf{2}_y, \mathbf{m}_z\} \times \{\mathbf{1}, 1' \times \bar{\mathbf{1}}\} \times \{\mathbf{1}, \mathbf{1}/[1/2, 1/2, 0]\} = \boldsymbol{Pmm'm} \times \{1, 1/[1/2, 1/2, 0]\}$

[c-] $Pmmm = \{\mathbf{1}, \mathbf{m}_x, \mathbf{m}_y, \mathbf{m}_z, \bar{\mathbf{1}}, \mathbf{2}_x, \mathbf{2}_y, \mathbf{2}_z\}$;

[d-] $Pm2m = \{\mathbf{1}, \mathbf{m}_x, \mathbf{2}_y, \mathbf{m}_z\}$;

[e-] $P2_1/n = \{\mathbf{1}, \mathbf{m}_z, \mathbf{2}_z/[1/2\ 1/2\ 0], \bar{\mathbf{1}}/[1/2\ 1/2\ 0]\}$;

[f-] $\boldsymbol{Pmm'm} = \{\mathbf{1}, \mathbf{m}_x, 1' \times \mathbf{m}_y, \mathbf{m}_z, 1' \times \bar{\mathbf{1}}, 1' \times \mathbf{2}_x, \mathbf{2}_y, 1' \times \mathbf{2}_z\} = Pm2m \times \{\mathbf{1}, 1' \times \mathbf{m}_y\}$;

[g-] $\boldsymbol{Pm2m} = Pm2m = \{\mathbf{1}, \mathbf{m}_x, \mathbf{2}_y, \mathbf{m}_z\}$;

[h-] $\boldsymbol{P2_1'/n} = \{\mathbf{1}, \mathbf{m}_z, 1' \times \mathbf{2}_z/[1/2\ 1/2\ 0], 1' \times \bar{\mathbf{1}}/[1/2\ 1/2\ 0]\} = \{\mathbf{1}, \mathbf{m}_z\} \times \{\mathbf{1}, 1' \times \mathbf{2}_z/[1/2\ 1/2\ 0]\}$;

Table 2. Crystallographic and magnetic parameters of YNi_4Si-type $NdNi_4Si$ at different temperatures: cell parameters *a*, *b* and *c*, unit cell volume *V*, $b/(3^{1/2}\bullet a)$ ratio, the atomic position of Ni1 atom y_{Ni1} [a-], $\mathbf{M}_b^{K0}$ the magnetic moments of Nd along the *b*-axis with $\mathbf{K}_0 = [0, 0, 0]$ wave vector. Reliability factors are: R_F for the crystal structure and R_F^m for the magnetic structure.

T (K)	Cell parameters	V (nm$_3$)	$b/(3^{1/2}\bullet a)$	y_{Ni1}	R_F (%)	Atom	M_b^{K0} (μ_B)	R_F^m (%)
298 [b-]	a = 0.51354(2) nm	0.16926(4)	0.93320(5)	0.3424(5)	4.5			
	b = 0.83006(3) nm							
	c = 0.39707(1) nm							
128	a = 0.51259(5) nm	0.16872(9)	0.93411(9)	0.3411(3)	3.6			
	b = 0.82933(9) nm							
	c = 0.39689(4) nm							
25	a = 0.51224(5) nm	0.16842(9)	0.93398(9)	0.3412(3)	3.4			
	b = 0.82865(9) nm							
	c = 0.39678(3) nm							
10	a = 0.51229(4) nm	0.16843(9)	0.93376(8)	0.3413(3)	3.6	Nd^1, Nd^2	0.97(12)	9.1
	b = 0.82854(7) nm							
	c = 0.39682(3) nm							
5	a = 0.51226(4) nm	0.16843(8)	0.93383(8)	0.3410(2)	3.1	Nd^1, Nd^2	2.26(6)	5.4
	b = 0.82855(7) nm							
	c = 0.39683(3) nm							
1.5	a = 0.51228(4) nm	0.16841(7)	0.93373(7)	0.3412(2)	3.0	Nd^1, Nd^2	2.37(5)	5.4
	b = 0.82849(6) nm							
	c = 0.39679(2) nm							

[a-] Atomic sites of YNi_4Si-type $NdNi_4Si$ (space group *Cmmm*): Nd (2*a*) [0, 0, 0], Ni1 (4*i*) [0, 0.3424(5), 0], Ni2 (4*f*) [1/4, 1/4, 1/2] and Si (2*c*) [0, 1/2, 1/2].

[b-] X-ray data.

Table 3. Magnetic properties of $CaCu_5$-type $NdNi_5$, $NdNi_4Si$ and YNi_4Si-type $NdNi_4Si$ compounds.

Compound	**Type structure**	**Θ_P** (K)	**M_{eff}** (μ_B/fu)	**T_C** (K)	**M_{sat}** (μ_B/fu)	**M_{res}** (μ_B/fu) (2 K)	**H_{coer}** (kOe) **(2 K)**	**ΔS_m** (J/kg·K) (0-50 kOe)	**Ref.**
$NdNi_5$	$CaCu_5$			7.2	2.1			-8.45	[14, 15]
$NdNi_4Si$	$CaCu_5$			9.2	1.5 (4.2 K, 90 kOe)	-	-	-7.3	[16]
$NdNi_4Si$	YNi_4Si	-21	3.8	12	1.1 (2 K, 50 kOe)	0.8	-3.0	-3.3	[a-]

[a-] This work.

Magnetic order and crystal structure study of YNi_4Si-type $NdNi_4Si$

Jinlei Yao, O. Isnard, A. V. Morozkin*, T.I. Ivanova, Yu. S. Koshkid'ko, A. E. Bogdanov, S. A. Nikitin, W. Suski

> Below ~12 K the YNi_4Si-type $NdNi_4Si$ shows a ferromagnetic ordering.

> MCE of $NdNi_4Si$ reaches value of –3.3 J/kg·K in 0-50 kOe near Curie point.

>$NdNi_4Si$ exhibits *b*-axis ferromagnetic order with the ***Cmm′m*** magnetic space group.

> Contrary to $CaCu_5$-type, YNi_4Si-type $NdNi_4Si$ shows hysteresis loop at 2 K.

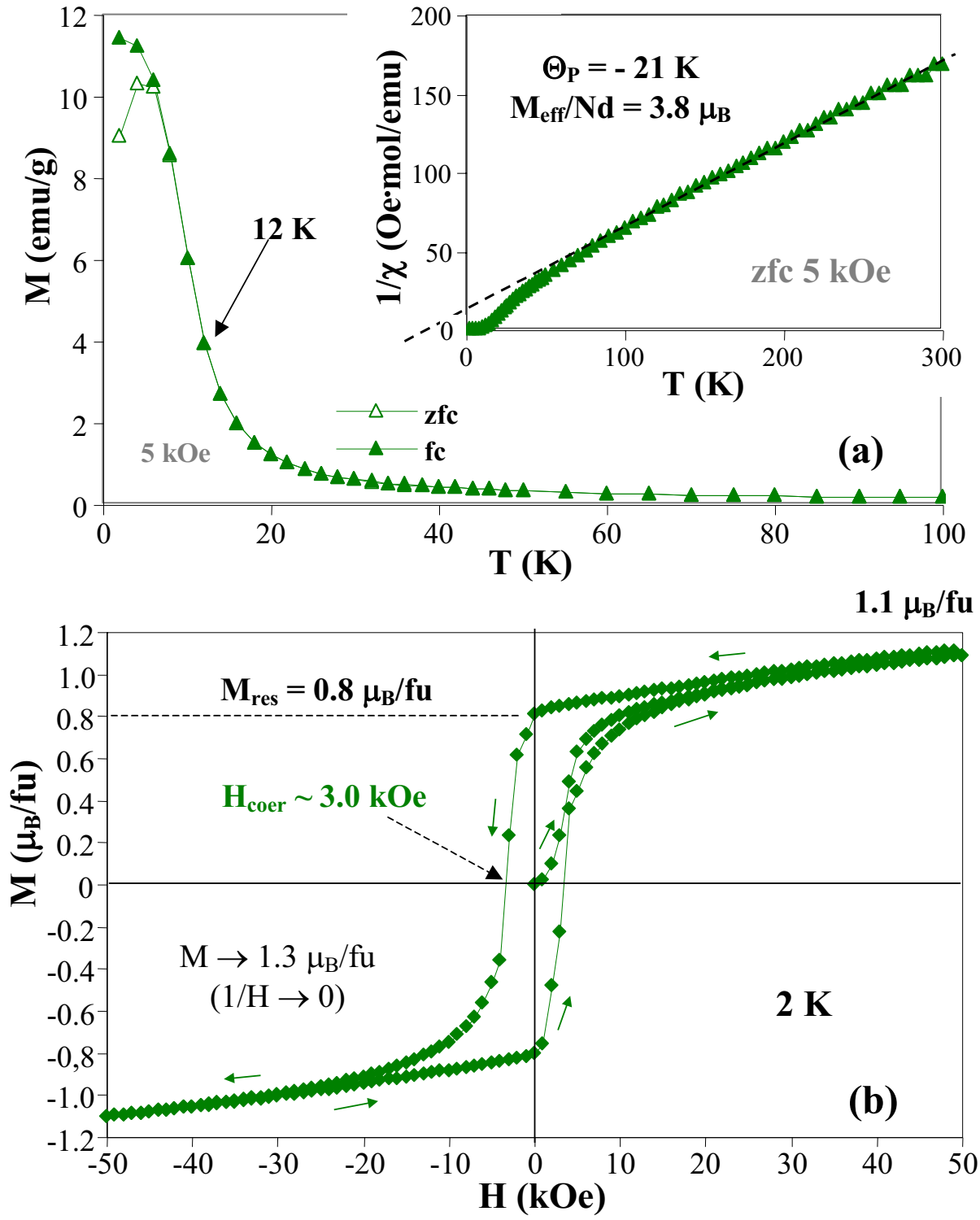

Fig. 1. (a) Magnetization and inverse magnetic susceptibility of $NdNi_4Si$ as a function of temperature in 5 kOe and (b) magnetisation vs. magnetic field of $NdNi_4Si$ at 2 K.

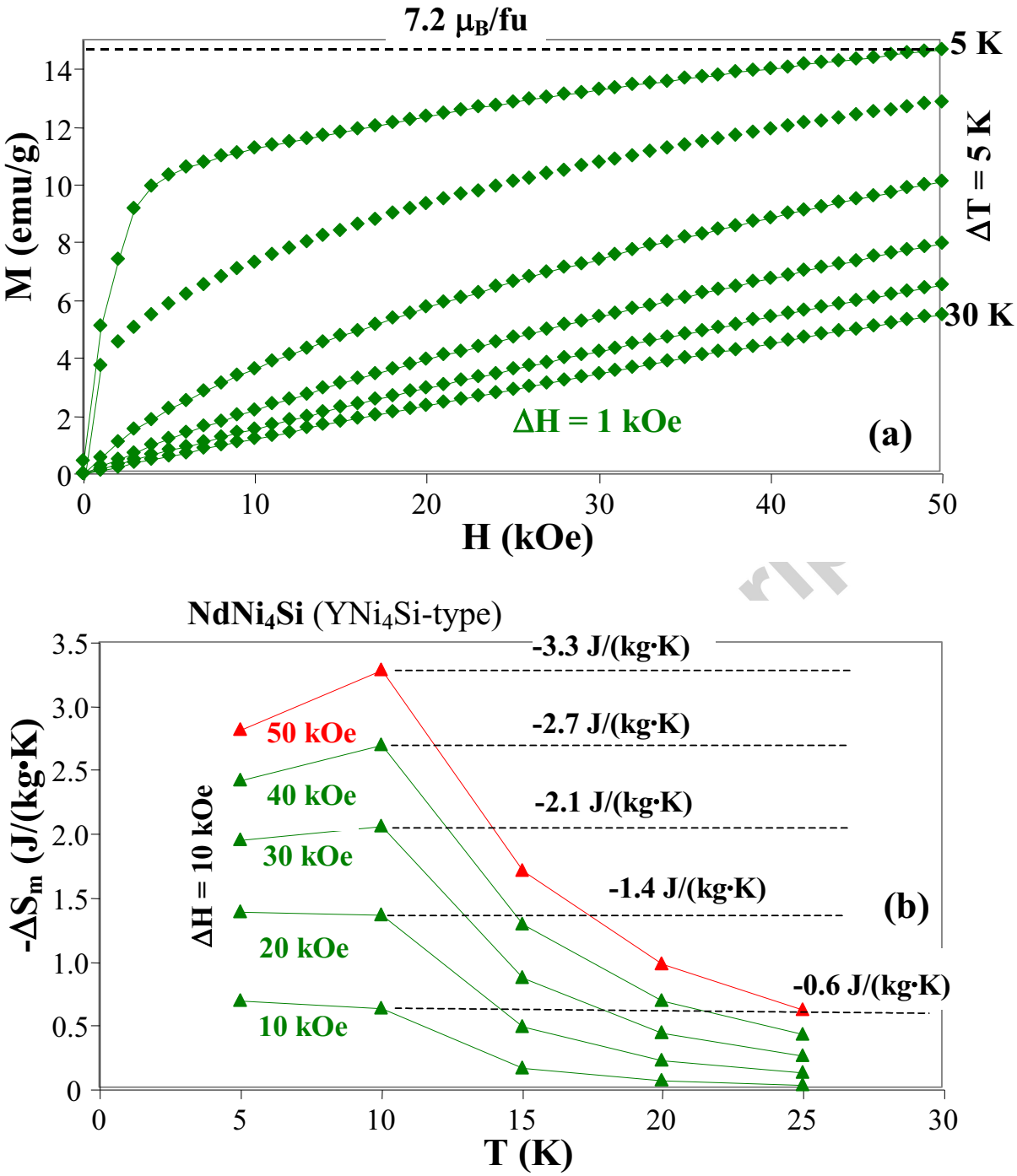

Fig. 2. (a) Magnetization vs. magnetic field and (b) the isothermal entropy change, $-\Delta S_m$, of $NdNi_4Si$ around the magnetic transition.

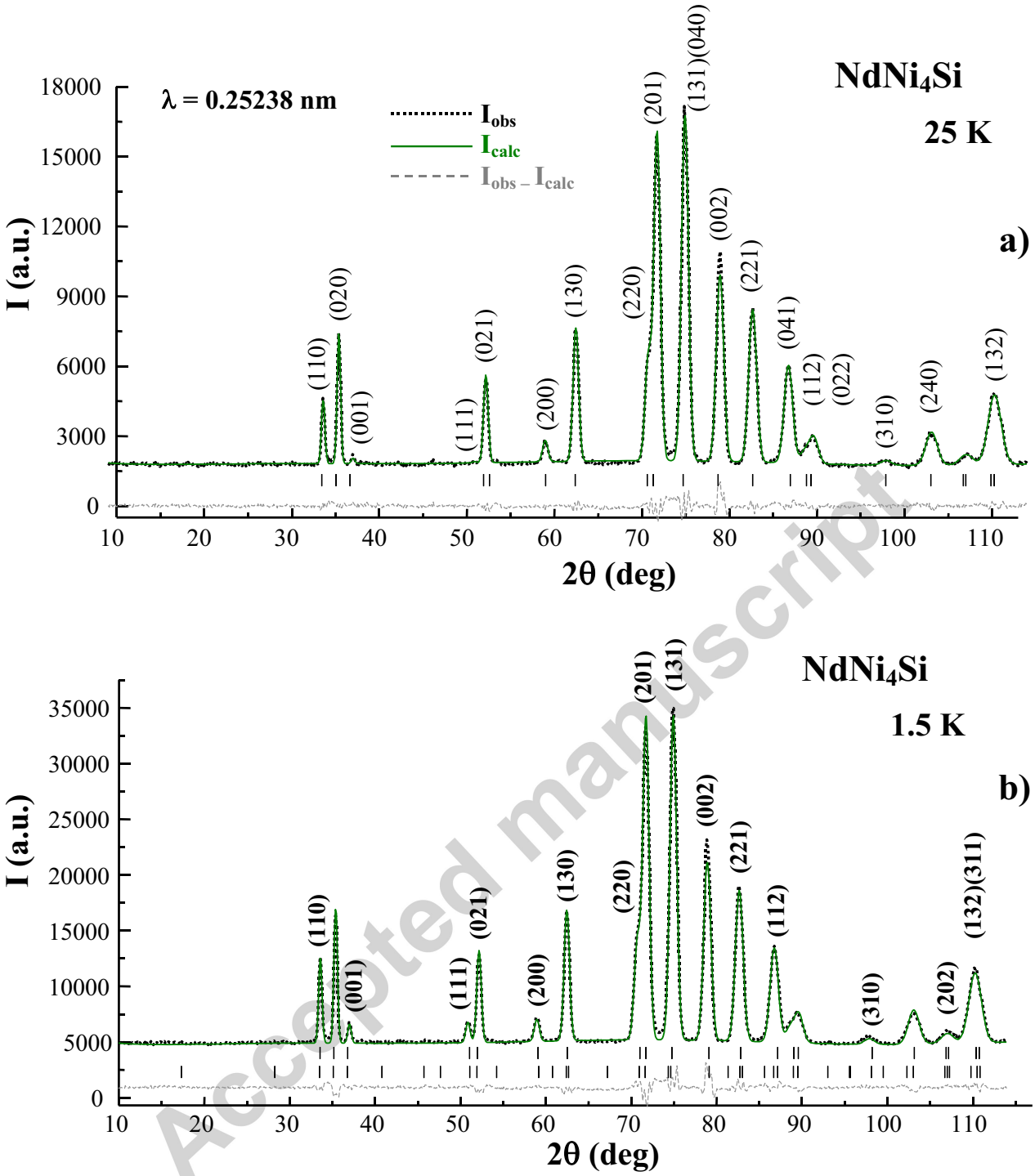

Fig. 3. Neutron diffraction patterns of $NdNi_4Si$ (a) at 25 K (paramagnetic state) and (b) at 1.5 K (*b*-axis ferromagnet with $\mathbf{K}_0$ = [0, 0, 0] wave vector. The first row of ticks refers to the nuclear Bragg peaks whereas the second row of lines refers to the magnetic reflections. The (hkl) of strongest magnetic reflections are indicated in **Figure 3b**.

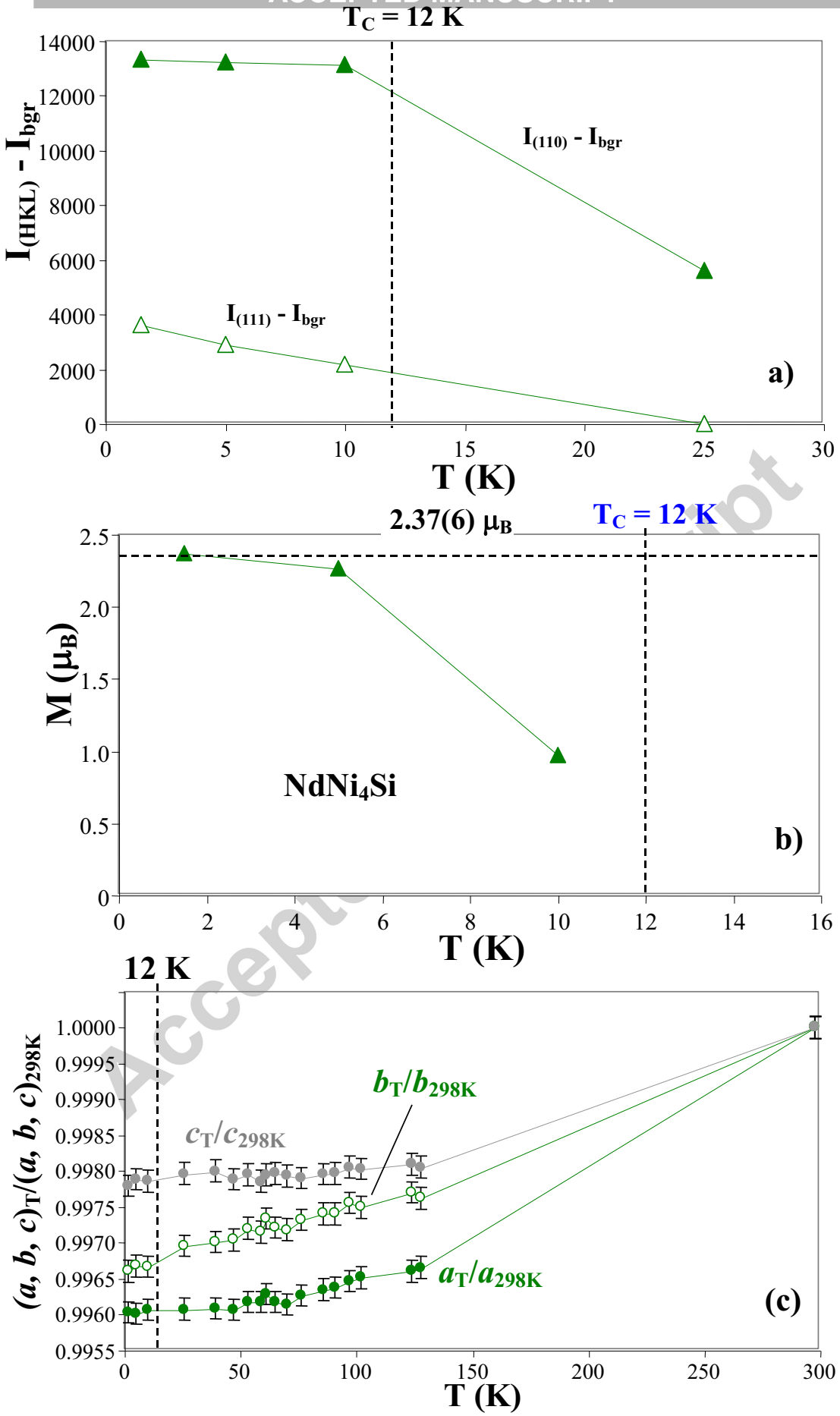

Fig. 4. Thermal evolution of (a) strongest magnetic reflections $I_{(HKL)}$ in the neutron diffraction patterns of $NdNi_4Si$, (b) the magnetic moments of Nd atom (along *b* axis) and (c) of relative cell parameters a_T/a_{298K}, b_T/b_{298K} and c_T/c_{298K}. Here a_T, b_T, c_T, a_{298K}, b_{298K} and c_{298K} are cell parameters of $NdNi_4Si$ at a given temperature T and 298 K, respectively.

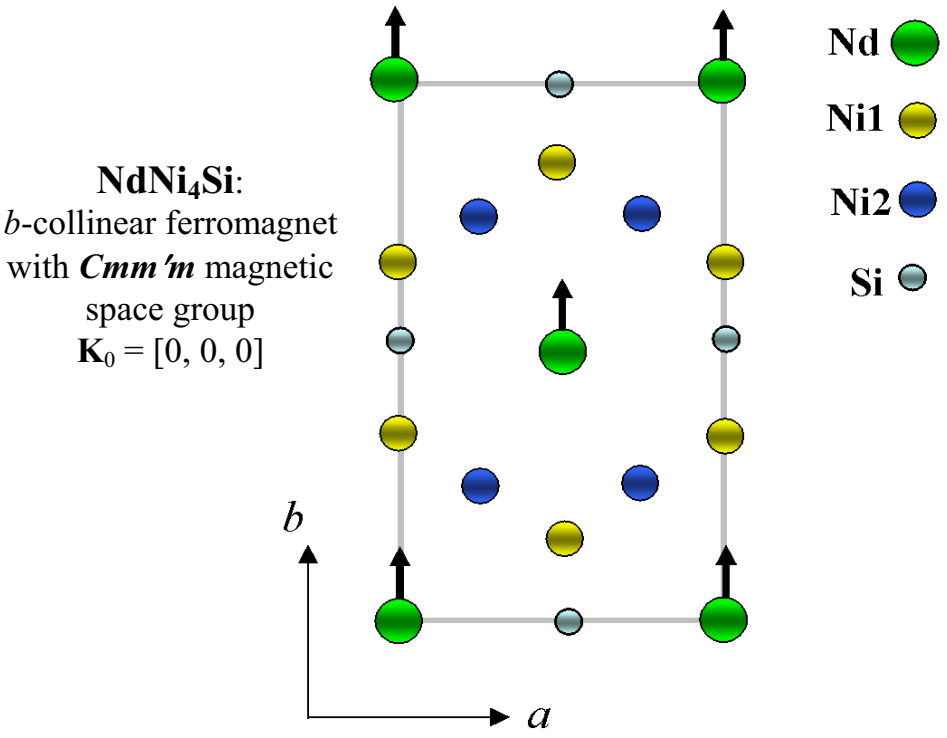

Fig. 5. The magnetic structure of YNi_4Si-type $NdNi_4Si$ with *b*-axis collinear ferromagnetic ordering of Nd sublattice below ~12 K of ***Cmm′m*** magnetic space group ($\mathbf{K}_0$ = [0, 0, 0] wave vector).

*Graphical Abstract (TOC Figure)

Magnetic order and crystal structure study of YNi_4Si-type $NdNi_4Si$

Jinlei Yao, O. Isnard, A. V. Morozkin*, T.I. Ivanova, Yu. S. Koshkid'ko, A. E. Bogdanov, S. A. Nikitin, W. Suski

$NdNi_4Si$:
b-collinear ferromagnet
with ***Cmm'm*** magnetic
space group
$\mathbf{K_0}$ = [0, 0, 0]
below **~12 K**

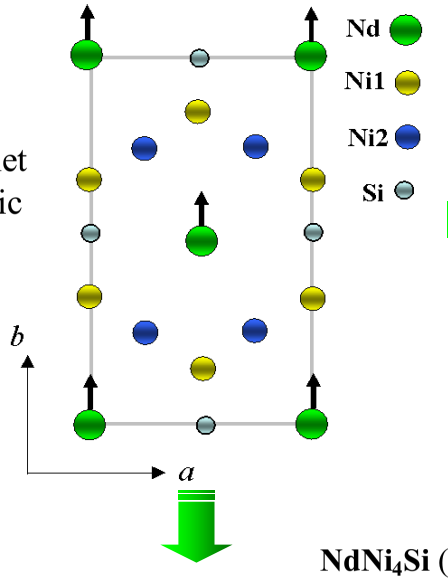

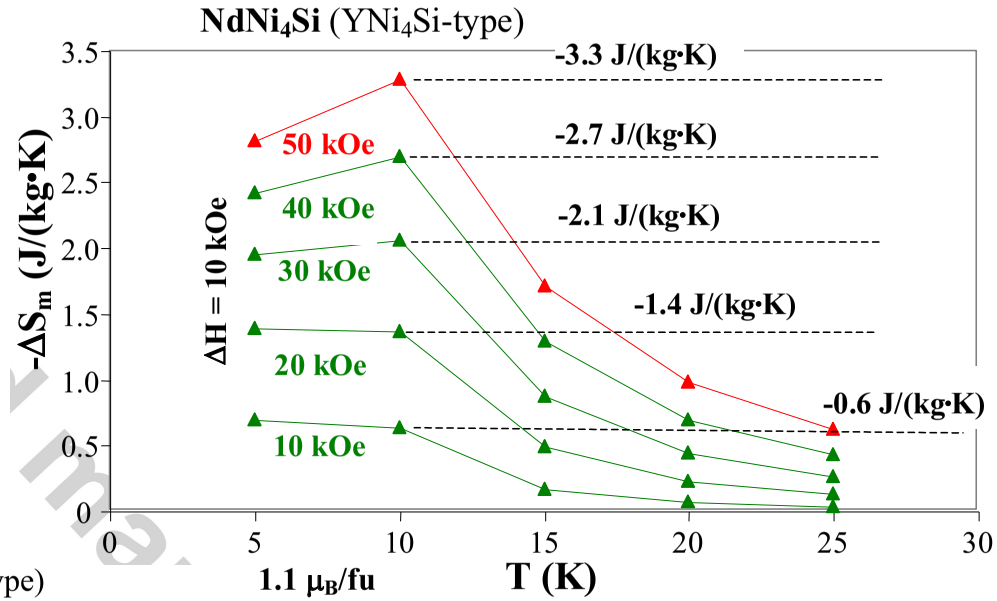

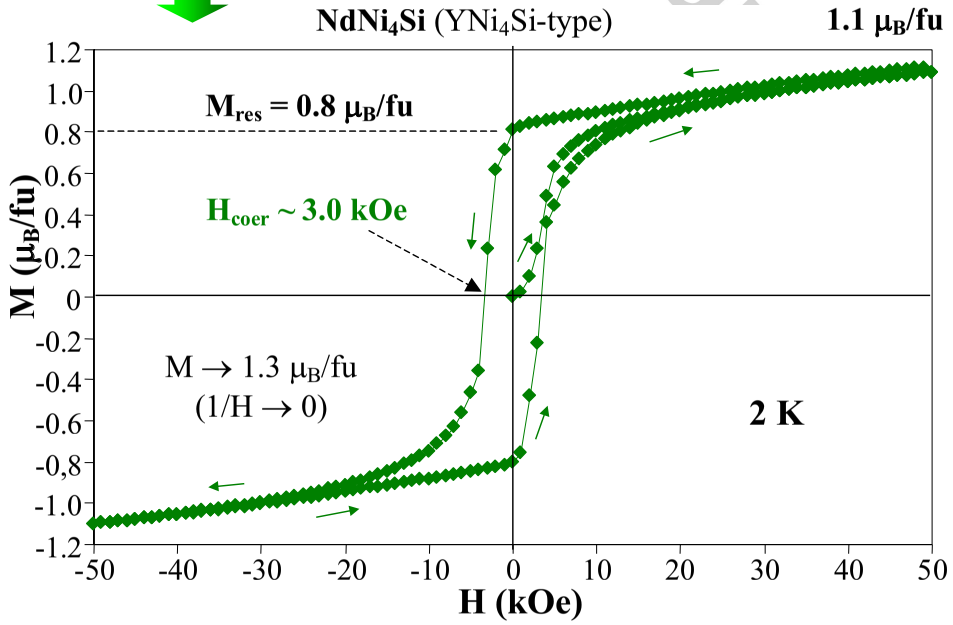

Magnetic order and crystal structure study of YNi_4Si-type $NdNi_4Si$

Jinlei Yao, O. Isnard, A. V. Morozkin*, T.I. Ivanova, Yu. S. Koshkid'ko, A. E. Bogdanov, S. A. Nikitin, W. Suski

The $NdNi_4Si$ supplement the series of the orthorhombic derivative of the $CaCu_5$-type, namely the YNi_4Si-type, RNi_4Si compounds (R = Y, La, Ce, Sm, Gd - Ho). Below ~12 K in a zero applied magnetic field, $NdNi_4Si$ exhibits a commensurate *b*-axis collinear ferromagnetic ordering with the ***Cmm′m*** magnetic space group. Compared to the $CaCu_5$-type $NdNi_4Si$ compound, the YNi_4Si-type counterpart has the relatively high ferromagnetic ordering temperature (9.2 K vs. 12 K), the small magnetocaloric effect (–7.3 J/kg·K vs. –3.3 J/kg·K for ΔH=50 kOe), and the large magnetic anisotropy at low temperatures. In contrast with $CaCu_5$-type $NdNi_4Si$, YNi_4Si-type $NdNi_4Si$ shows distinct hysteresis loop at 2 K.

We suggest that orthorhombic distortion may be used as a prospective route for optimisation of permanent magnetic properties in the family of $CaCu_5$-type rare earth materials.